Process Safety and Environmental Protection 146 (2021) 85–94

Contents lists available at ScienceDirect

Process Safety and Environmental Protection

journal homepage: www.elsevier.com/locate/psep

In-depth analyses of kinetics, thermodynamics and solid reaction mechanism for pyrolysis of hazardous petroleum sludge based on isoconversional models for its energy potential

Bineeta Singh, Satyansh Singh, Pradeep Kumar*

Department of Chemical Engineering and Technology, Indian Institute of Technology (Banaras Hindu University), Varanasi, 221 005, Uttar Pradesh, India

ARTICLE INFO

Article history:
Received 17 May 2020
Received in revised form 12 August 2020
Accepted 25 August 2020

Keywords:
Pyrolysis
Petroleum sludge
Iso-conversional method
Kinetic parameters
Solid reaction mechanism

ABSTRACT

The pyrolysis of hazardous petroleum sludge (PS) has widely been used for its remediation and energy extraction. However, in view of process optimization, scale-up, design and simulation, the kinetic (activation energy and frequency factor) and thermodynamic parameters (change in enthalpy (Δ H), entropy (Δ S), and Gibb's free energy (Δ G)) along with reaction mechanism followed by pyrolysis has rarely been investigated. Therefore, pyrolysis of PS was investigated in thermogravimetric analyzer (TGA) at three heating rates viz. 5, 10, 15 K min^{-1}. The kinetic and thermodynamic parameters were estimated by isoconversional methods such as Kissinger-Akahira-Sunose (KAS), Starink and Ozawa-Wall- Flynn (OWF) method. Further, solid reaction mechanism during pyrolysis was examined by employing Criado method (Z-master plot). The effect of heating rate on thermodynamic parameters and solid reaction mechanism was also examined. The average activation energy using Starink method was found to be 76.77 kJ mol^{-1}. The frequency factor, Δ H, Δ S and Δ G at 5 K min^{-1}, using activation energy from Starink method was found to be 3.23×10^7 sec^{-1}, 70.78 kJ mol^{-1}, -0.168 J mol^{-1} K^{-1}, and 189.88 kJ mol^{-1}, respectively. Z-master plot revealed that solid reaction mechanism depend on the degree of conversion and heating rate during pyrolysis of PS.

1. Introduction

The petroleum sludge (PS) which is generated from petroleum refining industries after recovery of oil from crude sources is considered as hazardous waste (Gong et al., 2020). The PS has been considered as a hazardous waste due to its lower ignition temperature, toxicity, mutagenicity and carcinogenicity (Cheng et al., 2018; Hu et al., 2017; Liu et al., 2009; Singh and Kumar, 2020). Every year around one billion tons of PS is generated from various sources associated with petroleum refining processes such as bottoms of oil tank, oil and water separator, and wastewater treatment plants (Hu et al., 2013; Liu et al., 2009; Qu et al., 2019). The PS has considerable quantity of combustible materials having high heating value (Choudhury et al., 2007). PS is a complex mixture of waste oil, wastewater, sand, organic and inorganic residue including variety of heavy metals (Qu et al., 2019). Inappropriate handling and disposal of PS can leads to severe threat to environmental and biological system (Chen et al., 2015a; Qu et al., 2019). Therefore, PS needs a proper effective and reasonable technique for their disposal. Due to its adverse impact on the environment, variety of processes such as biodegradation (Xu et al., 2014), pyrolysis (Chen et al., 2015c), solvent extraction (Al-Zahrani and Putra, 2013), membrane separation (Hu et al., 2013), incineration (Liu et al., 2010), ozonation (Zhong et al., 2003) has been tested from proper remediation and utilization of PS. However, these processes have certain constraints such as higher cost of operation, longer processing time, process efficiency, etc. (Xu et al., 2014).

Moreover, with rapid industrial development and ever increasing population of the world, the sources of energy can be considered as lifeblood for development of economy (Singh et al., 2019, 2020b). The total energy demand all around the world is increasing every year and it is predicted that it will increased around 28 % by 2040 (Kumar et al., 2020). The current oil sources are unable to provide the sufficient energy to the mankind and demand of energy is increasing day by day. The extraction of energy from waste may be a possible route for energy generation as well as waste remediation.

Among the various explored process for treatment of PS, the pyrolysis has gained dominance for energy recovery, utilization and remediation because of its fast and efficient nature (Singh et al., 2020a, c) and could convert waste PS into reusable energy source

* Corresponding author.
E-mail address: pkumar.che@iitbhu.ac.in (P. Kumar).

https://doi.org/10.1016/j.psep.2020.08.038
0957-5820/

with relatively lesser generation of secondary pollutants (Qu et al., 2019). Pyrolysis can be potential approach for converting recalcitrant and macro molecules of PS into relatively smaller molecules (Miao et al., 2019). Pyrolysis of PS brings four fold advantages: (1) the reuse of PS can minimize the contamination of hazardous waste with environment as a result of careless handling and disposal; (2) the pyrolysis oil obtained from the pyrolysis of PS can offset the extra pressure on demand and supply chain of fossil derived fuels such as petroleum and diesel; (3) huge amount of PS generated every year, thus as a raw material for pyrolysis it is readily available and inexpensive; (4) the study of pyrolysis will facilitate the other thermochemical conversion processes such as combustion or gasification, since, pyrolysis is the initial stage of combustion or gasification (Qu et al., 2019). As compared to other treatment processes, pyrolysis can be promising technique for sludge management due to its ability to recover pyrolysis oil and gaseous products as well as its fast and efficient nature. Pyrolysis also leads to reduction in solid waste and less secondary pollution. Pyrolysis can recovered around 80 % of total organic carbon present in sludge (Liu et al., 2009). The gaseous products from pyrolysis of petroleum sludge can be used for heating purpose. The pyrolysis oil obtained has similar properties to low grade petroleum distillate and can directly be sued as fuel in boiler, furnaces and engines. The solid waste generated during pyrolysis of sludge can be used as adsorbent for wastewater treatment (Jiang et al., 2018; Premarathna et al., 2019; Tian et al., 2020).

The assessment of kinetics and thermodynamics along with reaction mechanism followed by pyrolysis of a feedstock is very crucial for optimization of process parameters, scale up and design of pyrolysis reactor system (Bach and Chen, 2017; Choudhury et al., 2020). As per the recommendations given by the kinetic committee of the International Confederation for Thermal Analysis and Calorimetry (ICTAC), the methods developed on the basis of thermogravimetric analysis (TGA) are the most accurate and prevalent for study of thermochemical decomposition of various feedstocks such as biomass (Singh et al., 2020c), lignite (Chen et al., 2015b), sewage sludge (Soria-Verdugo et al., 2017) and oil sludge (Qu et al., 2019). The pyrolysis of PS is a complex and multi-step process as a result large variation in activation energy with conversion is observed. This problem can be assessed by using iso-conversional model (Cheng et al., 2018). The iso-conversional method can demonstrate the complexity of pyrolysis process based on relationship between activation energy and conversion without following any specific kinetic reaction model (Vyazovkin et al., 2011). Based on the mass loss data in the form of TGA and DTG, the kinetic parameters can be calculated using isoconversional models. Then, thermodynamic parameters can be calculated by employing kinetic parameters (Singh et al., 2020c).

Pyrolysis of PS using thermogravimetric analysis followed by estimation of kinetic parameters has been investigated by many researchers. For instance, Miao et al. (Miao et al., 2019) investigated the kinetic parameters for pyrolysis oil field sludge using iso-conversional methods. Ma et al. (Ma et al., 2019) estimated the kinetic parameter using distribution activation energy model (DEAM) and effect of heating rate on the pyrolysis of oil-field sludge. Qu et al. (Qu et al., 2019) investigated the effect of solid content on the pyrolysis behavior of oily sludge by estimation of kinetic parameters and solid reaction mechanism. Choudhury et al. (Choudhury et al., 2007) examined the non-isothermal degradation kinetics of pyrolysis of petroleum refinery sludge based on iso-conversional models. Liu et al. (Liu et al., 2009) investigated the kinetic parameters for pyrolysis of oil sludge using model-free kinetic analysis. From the literature it was found that kinetic parameters such as activation energy and order of reaction has been successfully examined by many researchers based on iso-conversional model and independent parallel reaction model. However, estimation and effect of heating rate during pyrolysis on thermodynamic parameters such as change in enthalpy (Δ H), change in entropy (Δ S), and change in Gibb's free energy (Δ G) for pyrolysis of PS has not been reported so far. In addition, solid reaction mechanism followed during pyrolysis of PS needed further clarification based different range of conversion of PS and heating rate during pyrolysis.

Therefore, present work was aimed to investigate the kinetic parameters (activation energy, frequency factor), thermodynamic parameters (change in enthalpy (Δ H), change in entropy (Δ S), and change in Gibb's free energy (Δ G)) and solid reaction mechanism during pyrolysis of PS. Three iso-conversional methods such as, Kissinger-Akahira-Sunose (KAS), Starink and Ozawa-Wall-Flynn (OWF) method were used to calculate the kinetic and thermodynamic parameters. Further, solid reaction mechanism during pyrolysis was examined by employing Criado method (Z-master plot). Also, the physicochemical properties of PS were studied by using proximate, ultimate and ICP-OES analyses.

Table 1
Physicochemical properties of petroleum sludge.

Properties	Petroleum sludge (PS)	ASTM Standard
Proximate analysis		
Moisture content (wt%)[a]	21.41	ASTM D 3173
Volatile matter (wt%)	63.33	ASTM D 3174
Fixed carbon (wt%)[b]	11.84	–
Ash content (wt%)	3.78	ASTM D 3175
Ultimate analysis		
C (wt%)	50.39	–
H (wt%)	7.09	–
N (wt%)	1.66	–
O (wt%)[b]	37.38	–
S (wt%)	3.48	–
HHV (MJ kg^{-1})	12.42	ASTM D 5685–10A

[a] As received.
[b] Calculated by difference.

2. Materials and methods

2.1. Collection and characterization of petroleum sludge

The oily petroleum sludge examined in this work was obtained from petroleum refinery situated in north India. The collected PS sample was placed in a cold room maintained at 4 °C to preserve its original properties. Before experiments it was dried in hot air oven at 70 °C for 2 h. Then it was placed in air tight container to avoid the variation in properties of sludge. The PS was subjected to proximate, ultimate, and induced coupled plasma spectroscopic analysis. The moisture content (MC), ash content (AC) and volatile matter (VM) was estimated by following the standard ASTM methods mentioned in Table 1. The fixed carbon of PS was estimated by difference (100 – (MC + VM + AC)). The elemental analysis for carbon, nitrogen, hydrogen and sulphur was carried out by CHNS analyzer (Euro vector EA element analyzer). The oxygen was estimated by difference (100 – (C + H + N + S)). The higher heating value of PS was estimated by employing bomb calorimeter (RSB3, Rajdhani Scientific inst. Co., India). The metal present in PS was analysed by inductively coupled plasma optical emission spectrometry (ICP-OES) analyzer (iCAP 7400 Thermo Fisher Scientific, India). Metals concentration in the PS was analyzed using acid digestion of the dried sludge according to US EPA method 3050B. The PS was digested prior to ICP-OES analysis. 5 g of sample was digested with 7 mL of 65 % HNO_3 and 1 mL of 30 % H_2O_2 in a microwave oven digester 95 ± 5 °C. The final sample was passed through 0.22 μm syringe filter before metal testing.

2.2. Thermogravimetric analysis of PS

The TGA analyzer (NETZSCH TG 209F1 Libra) was used to perform the pyrolysis. The dried PS sample (approximately 5 ± 0.2 mg in each case) was kept in alumina crucible and heated from ambient to 1273 K at 5, 10, 15 K min^{-1}, respectively. The high purity nitrogen gas (99.999 %) at 100 mL min^{-1} was passed to maintain the inert atmosphere. The high flow rate of nitrogen and small sample weight was considered to prevent the secondary cracking of non-condensable gases and to overcome the heat and mass transfer limitations, respectively, (Chen et al., 2015a). Before the start of experiments, blank run was performed to obtain the TG base line to offset the effect of buoyancy (Chen et al., 2015a; Qu et al., 2019). Further analysis was executed based on recorded data of TGA and differential thermogravimetric analysis (DTG). The precision in the measurement of temperature and sensitivity of microbalance of TGA was ± 1 K and ± 0.1 μ g, respectively. The TGA analysis was replicated twice to reduce the experimental error.

2.3. Kinetic study

The pyrolysis of PS is complex process which is accompanied by series of complex reactions occurring simultaneously during pyrolysis. However, the mathematical model could be used to describe the pyrolysis process based on superposition of different reaction among different phases (Qu et al., 2019). The general solid-state reaction for pyrolysis of PS can be written as follows:

$$\text{Solid fuel(PS)} \xrightarrow{k} \text{Volatile matter (Gases and Tar)} + \text{Char} \quad (1)$$

A general expression for conversion of PS during pyrolysis can be defined as follows:

$$\frac{d\alpha}{dt} = k(T) f(\alpha) \quad (2)$$

where, $\frac{d\alpha}{dt}$ is the conversion rate, k is the pyrolysis rate constant, α is the degree of conversion, t is the time for pyrolysis reaction, T is the absolute temperature, $f(\alpha)$ is the reaction model in differential form.

The conversion of PS during pyrolysis can be described as follows:

$$\alpha = \frac{w_0 - w_t}{w_0 - w_f} \quad (3)$$

where, w_0, w_t, w_f are the weight of PS sample recorded by TGA analyzer at start of the run, time t and end of the run, respectively.

The rate constant for pyrolysis of PS is dependent on temperature and relationship can be written as follows:

$$k(T) = Ae^{\frac{-Ea}{RT}} \quad (4)$$

where E_a and A are the kinetic parameters, signifying the activation energy and frequency factor, respectively. R signifies the universal gas constant.

The final equation for pyrolysis of PS can be obtained by joining Eqs. (2) and (4). Eq. (5) represent the fundamental relationship which can be applied to calculate the activation energy during pyrolysis of PS.

$$\frac{d\alpha}{dt} = Ae^{\frac{-Ea}{RT}} f(\alpha) \quad (5)$$

The constant value of heating rate at which thermogravimetric analysis was performed can be expressed as:

$$\beta = \frac{dT}{dt} \quad (6)$$

The temperature during TGA varied with heating rate. Using Eq. (6) the rate of conversion can be presented into temperature derivative. Therefore,

$$\frac{d\alpha}{dT} = \frac{d\alpha}{dt}\frac{dt}{dT} \quad (7)$$

$$\frac{d\alpha}{dT} = \frac{d\alpha}{dt}\frac{1}{\beta} \quad (8)$$

Eq. (9) can be obtained with the help of Eqs. (5) and (8)

$$\frac{d\alpha}{dt} = \frac{A}{\beta} e^{\frac{-Ea}{RT}} f(\alpha) \quad (9)$$

The Eq. (9) is referred as differential form of kinetic equation which is used during estimation of kinetic parameters using model based on differential form. After integration of Eq. (9) on both sides the Eq. (10) can be deduced as:

$$g(\alpha) = \int_0^{\alpha} \frac{d\alpha}{f(\alpha)} = \frac{A}{\beta}\int_{T_0}^{T} \exp\left(-\frac{E_a}{RT}\right) dT \quad (10)$$

The Eq. (10) is referred as integral form of kinetic equation which is used during estimation of kinetic parameters using model based on integral form, where, g (α) represents function of conversion in integral form. $f(\alpha)$ represents the algebraic forms of expressions related to physical models which illustrates the solid state reaction mechanism during pyrolysis. The expressions of $f(\alpha)$ and $g(\alpha)$ depict the various reaction mechanism are presented in Table S1 (Supplementary material). With the help of these expressions, mechanism followed during pyrolysis was predicted. In this work, the activation energy was calculated by employing three iso-conversional methods, such as KAS, OWF and Starink method.

2.4. Model-free methods (isoconversional models)

2.4.1. The Kissinger-Akahira-Sunose (KAS) method

KAS method predicted the relationship between heating rate and activation energy through non-isothermal linear integral as per the Eqs. (11) (Aboulkas and El Harfi, 2008; Heydari et al., 2015).

$$\ln\left(\frac{\beta}{T_\alpha^2}\right) = \ln\left(\frac{AR}{E_\alpha g(\alpha)}\right) - \frac{E_a}{RT_\alpha} \quad (11)$$

where T_α is the temperature at conversion α. The plot between ln $\left(\frac{\beta}{T_\alpha{}^2}\right)$ and $\frac{1}{T_\alpha}$, at a constant value of conversion gives a straight line, whose slope can be used to calculate activation energy.

2.4.2. The Ozawa-Wall- Flynn (OWF) method

OWF method can be derived by integrating Eq. (9), and then Doyle's approximation was implied over temperature integral. The resulting equations are obtained as Eqs. (12) and (13) (Chen et al., 2018; Heydari et al., 2015). At every conversion three points for ln β and $\frac{1}{T_\alpha}$ can be obtained at three heating rates. The plot between these points will give a straight line having slope $(-1.052\frac{E_a}{R})$ which can be used to compute activation energy.

$$\ln\beta = \ln\left(\frac{AE_a}{Rg(\alpha)}\right) - 5.3305 - 1.052\frac{E_a}{RT_\alpha} \quad (12)$$

or

$$\ln\beta = \ln\left(\frac{0.0048AE_a}{Rg(\alpha)}\right) - 1.052\frac{E_a}{RT_\alpha} \quad (13)$$

2.4.3. Starink method

Starink analyzed the KAS and OWF methods to get the following equation (Cheng et al., 2018).

$$\ln\left(\frac{\beta}{T_\alpha^S}\right) = C - \frac{BE_a}{RT_\alpha} \tag{14}$$

where, S and B take different values. By using temperature integral approximation, Starink obtained the value of S and B as 1.92, and 1.0008, respectively. Then Eq. (14) can be rewritten as:

$$\ln\left(\frac{\beta}{T^{1.92}}\right) = C - 1.0008\frac{E_a}{RT_\alpha} \tag{15}$$

At every conversion, three points for $\ln\left(\frac{\beta}{T^S}\right)$ and $\frac{1}{T_\alpha}$ can be obtained at three heating rates. The plot between these points will give a straight line having slope, $(-1.0008\frac{E_\alpha}{R})$ which can be used to compute activation energy.

2.5. Determination of reaction kinetic model

Once the activation energy was determined, the Criado method (Z-master plot) was employed to describe the kinetic model followed during pyrolysis of PS. The Criado method is described by Eq. (19) (Criado, 1978). The Z-master plot can be of three types namely, integral, differential and combination of both (Alam et al., 2020; Gotor et al., 2000). The Z-Master plot $Z(\alpha)$ can be deduced by multiplication of both integral and differential of reaction kinetic model (Alam et al., 2020). At atmospheric temperature, the decomposition of PS is very less. Therefore, limit (T_o) in the integral expression (Eq. 10) can be approximated to zero. After rearrangement and approximation of limit the integral expression (Eq. 10) can be written as:

$$g(\alpha) = \int_0^\alpha \frac{d\alpha}{f(\alpha)} = \frac{A}{\beta}\int_{T_0}^{T} \exp\left(-\frac{E_a}{RT}\right)dT = \frac{A}{\beta}\int_0^{T} \exp\left(-\frac{E_a}{RT}\right)dT$$
$$= \frac{AE}{\beta R}(p(u)) \tag{16}$$

In Eq. (16) p(u) is the integral term associated with temperature. Also, the analytical solution of Eq. (16) is not possible. Therefore, by assuming pyrolysis of PS as single step process, and with constant value of g (α), the analysis of Z-master plot provides a diverse choice for selection of suitable kinetic model. Considering $\alpha = 0.5$ as reference point, the Eq. (16) can be written as:

$$g(0.5) = \frac{AE}{\beta R}(p(u_{0.5})) \tag{17}$$

where $u_{0.5} = \frac{E}{RT_{0.5}}$. After dividing the Eq. (16) by Eq. (17), we can get the expression as:

$$\frac{g(\alpha)}{g(0.5)} = \frac{p(u)}{p(u_{0.5})} \tag{18}$$

$$\frac{Z(\alpha)}{Z(0.5)} = \frac{f(\alpha)\times g(\alpha)}{f(0.5)\times g(0.5)} = \left(\frac{T_\alpha}{T_{0.5}}\right)^2 \times \frac{(d\alpha/dT)_\alpha}{(d\alpha/dT)_{0.5}} \tag{19}$$

The left-hand side of Eq. (19) was used for generation of Z-master plots for theoretical solid reaction mechanism as mentioned in Table S1. While, the term in right-hand side $((T_\alpha/T_{0.5})^2 \times ((d\alpha/dT)_\alpha/(d\alpha/dT)_{0.5}))$ was used to generate experimental Z-master plot (Alam et al., 2020; Singh et al., 2020c). The value of left-hand side term $((Z(\alpha)/Z(0.5))$ at reference point ($\alpha = 0.5$) for all theoretical curve is one at which all the theoretical curve converge (Singh et al., 2020c). The most appropriate model followed during the pyrolysis of PS was obtained by matching the experimental and theoretical Z-master plot. The model at which corresponding experimental and theoretical Z-master plots are closest to each other will be followed during pyrolysis of PS (Dhyani et al., 2017; Mishra et al., 2015; Poletto et al., 2012).

2.6. Calculation of thermodynamic parameter

The activation energy was calculated by employing three isoconversional methods, such as KAS, OWF and Starink method. The frequency factor at different conversion was calculated by using Kissinger method represented by Eq. (20). By using activation energy the frequency factor can be obtained by using Eq. (21) at different conversion. Based on the activation energy from Starink method frequency factor was calculated. Since ICTAC has recommended the Starink method as one of the most accurate isoconversional method (Cheng et al., 2018).

$$\ln\left(\frac{\beta}{T_p^S}\right) = \ln\left(\frac{AR}{E}\right) - \frac{E}{RT_p} \tag{20}$$

$$A = \beta.E_\alpha.\mathrm{Exp}\left(\frac{E_\alpha}{RT_p}\right)/\left(R.T_p^2\right) \tag{21}$$

where, T_p, is the DTG peak temperature, β is the heating rate, E_α is the activation energy at different conversion, and R is gas constant.

With the help of obtained value of activation energy and frequency factor, change in enthalpy, Gibbs free energy and entropy can be obtained at different value of conversion by employing Eqs. (22)–(24).

$$\Delta H = E_\alpha - RT_\alpha \tag{22}$$

$$\Delta G = E_\alpha + R.T_p.\ln\left(\frac{K_B.T_\alpha}{h.A}\right) \tag{23}$$

$$\Delta S = \frac{\Delta H - \Delta G}{T_p} \tag{24}$$

where, T_α represents temperature at different conversion varying from 0.1 to 0.9, T_p represents the DTG peak temperature, K_B represents the Boltzmann constant ($1.381*10^{-23}$ J K^{-1}), and h represents the Plank constant ($6.626*10^{-23}$ J s).

3. Results and discussion

3.1. Physicochemical characteristics of PS

The physicochemical properties of PS obtained from proximate analysis (moisture content, fixed carbon content, volatile matter and oxygen content), ultimate analysis (C, H, O, N and S) are presented in Table 1 and result of ICP-OES analysis are presented in Table 2.

3.2. Pyrolysis behavior of PS

The pyrolysis behavior of PS was investigated using Thermogravimetric analyzer and the results are exhibited as TGA (Fig. 1a) and DTG (Fig. 1b). For detailed analysis of pyrolysis process the DTG curves at different heating rates were divided into three distinct stages based on the occurrence DTG peaks (Gong et al., 2018). Each stage during pyrolysis has its own significance. The first stage (300–400 K) corresponds to removal of surface and bound moisture from the PS sample with lesser weight loss as compared to other stages (Gong et al., 2020). The intensity of peak in stage 1 is small because PS sample was dried for 24 h at 105 °C before carrying out the TGA experiments. The second stage (400–1000 K) ascribed the major devolatilization zone where maximum weight loss occurred due to decomposition of lighter, medium and heavy molecular weight volatile compounds present

Table 2
Elements detected from ICP-OES of the petroleum sludge.

Elements	Fe	Ca	Mg	Cu	Cd	Cr	Pb	Zn	Ti
wt% (ppm)	357.2	100	40	35	42.5	105	198	580	547
Elements	Ni	Co	As	V	Mn	K	Ba	B	Al
wt% (ppm)	240	16	13.5	72	4.24	3.38	ND	0.01	26.40

ND; Not detected.

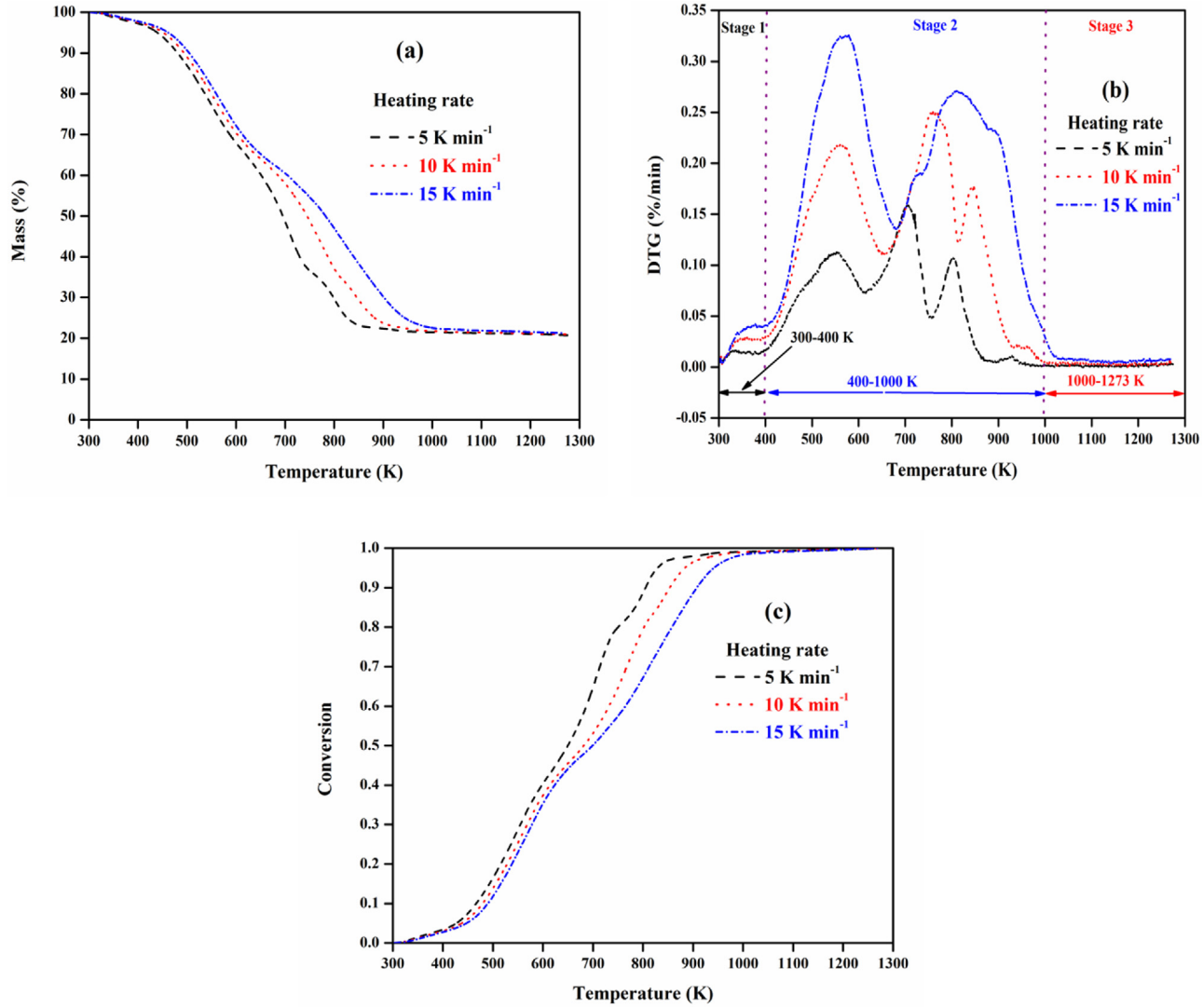

Fig. 1. **(a)** TGA; **(b)** DTG; **(c)** Conversion of PS during pyrolysis at different heating rates.

in PS. The stage 3 (1000–1273 K) associated with char formation and simultaneous occurrence of secondary cracking reactions as well as decomposition of inorganic mineral present in PS. It was also observed that overlapping phenomenon occurred between different stages (Qu et al., 2019). Meanwhile, thermal hysteresis phenomenon was also observed with increase in heating rate during pyrolysis of PS (Qu et al., 2019). Due to thermal hysteresis, the TGA and DTG profile shifted to higher temperature zone with increase in heating rate. Heat and mass transfer limitations are mainly responsible for thermal hysteresis phenomenon. Thus increase in heating rate during pyrolysis speed up the pyrolysis process and increases the rate of weight loss. These results are consistent with published literature about pyrolysis of oily sludge (Gong et al., 2020, 2018; Qu et al., 2019). The degree of conversion of PS is defined as the fraction of PS which decomposed at particular time. Fig. 1c exhibited the conversion of PS at different heating rate. It is evident from the result that with increase in heating rate during pyrolysis, the same degree of conversion was achieved at higher temperature. With increase in heating rate, the PS sample experienced a stronger thermal shock in lesser time. As a result same degree of conversion achieved at higher temperature. The gradual heating of PS will facilitate the higher degree of conversion

3.3. Estimation of activation energy

The activation energy is defined as the minimum energy essential for occurrence of a reaction. It can also be used for predicting the quality of fuel. The fuel having high activation energy consumes longer time to form activated complex for proceeding of

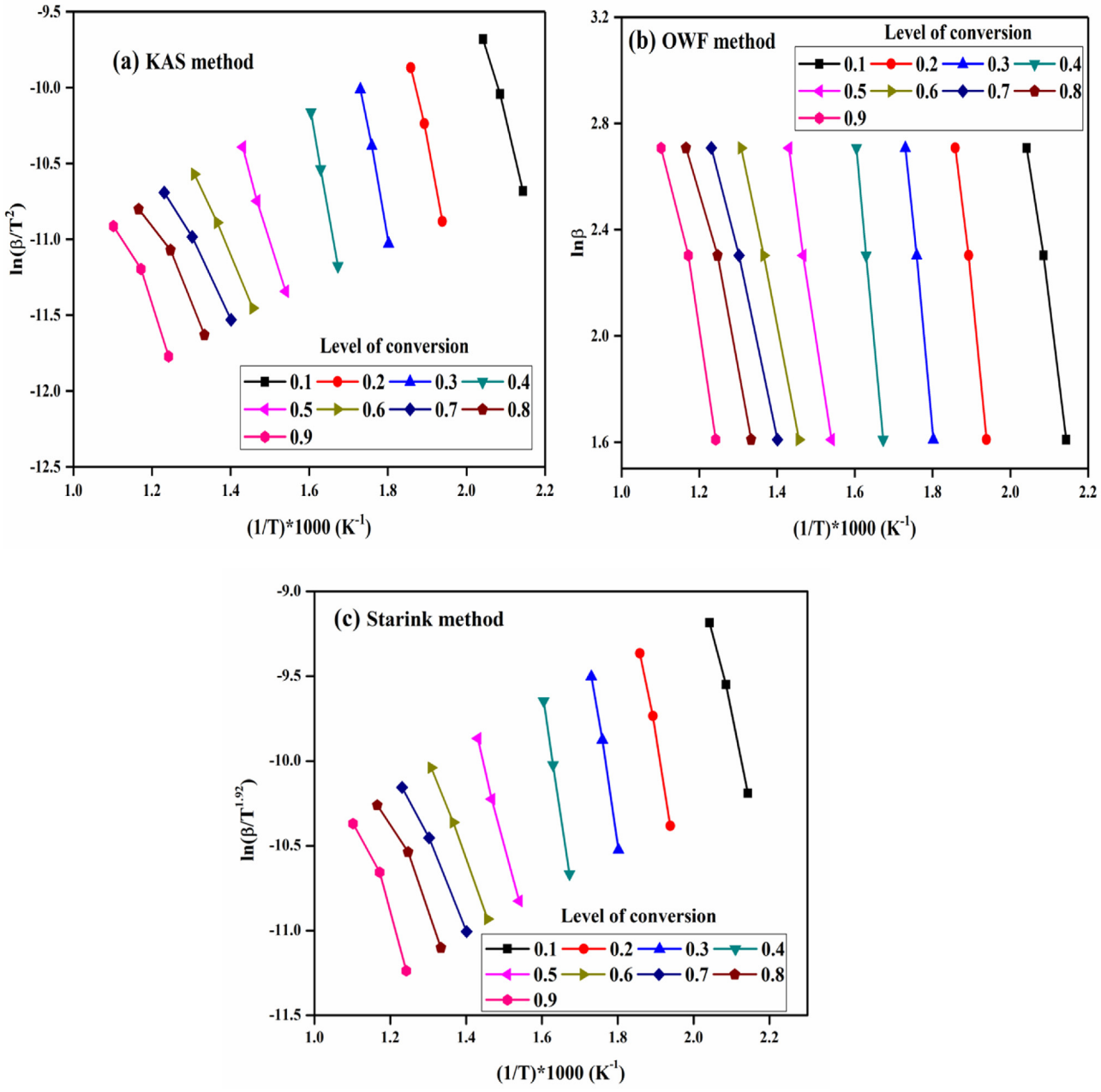

Fig. 2. Iso-conversion models for kinetic analysis of PS **(a)** KAS; **(b)** OWF; **(c)** Starink methods.

Table 3
Activation energy for pyrolysis of PS at different conversion using iso-conversional model.

Conversion	KAS method		OWF method		Starink method	
	E (kJ mol^{-1})	R^2	E (kJ mol^{-1})	R^2	E (kJ mol^{-1})	R^2
0.1	71.870	0.9978	90.691	0.9951	83.150	0.9942
0.2	105.471	0.9949	114.597	0.9957	106.164	0.9949
0.3	118.425	0.9977	128.251	0.9981	119.184	0.9977
0.4	123.313	0.9999	133.890	0.9999	124.122	0.9999
0.5	82.563	0.9942	83.319	0.9983	72.552	0.9979
0.6	49.578	0.9989	61.797	0.9994	50.222	0.9989
0.7	41.367	0.9938	54.172	0.9968	42.008	0.9939
0.8	41.308	0.9679	54.808	0.9826	41.977	0.9688
0.9	50.900	0.9628	65.315	0.978	51.634	0.9636
Average	**76.088**	**0.9897**	**87.426**	**0.9937**	**76.779**	**0.9899**

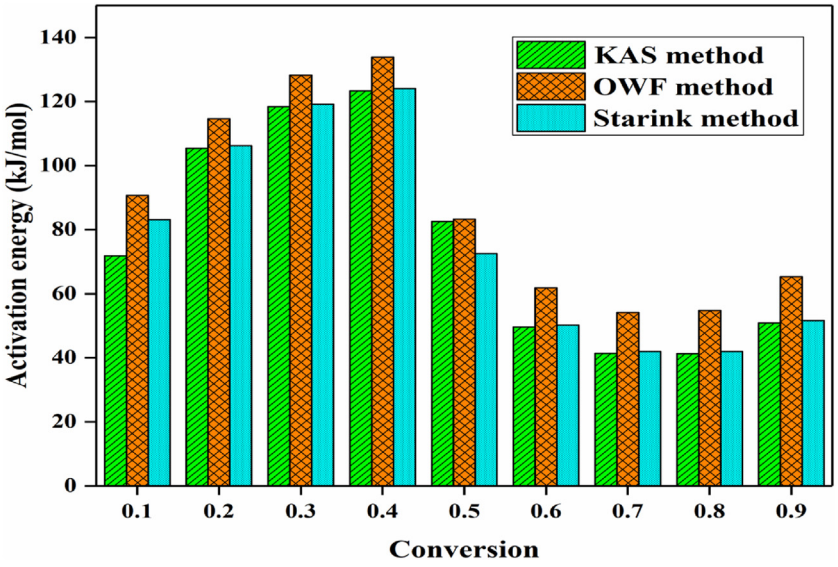

Fig. 3. Variation of activation energy of PS for different using different iso-conversion models.

Table 4
Comparison of activation energy for pyrolysis of PS form published literature based on iso-conversional models.

Feedstock	Activation energy (kJ mol^{-1})					References
	KAS method	OWF method	Starink method	Friedman method	CR method	
Petroleum sludge	84.44	95.19	–	102.77	–	(Choudhury et al., 2007)
Oil sludge	–	–	82.4	84.7	–	(Cheng et al., 2018)
Oil sludge	45.93	53.37	–	–	–	(Qu et al., 2019)
Oil-field sludge	–	245.74	–	–	102.98 (at 10 K min^{-1})	(Miao et al., 2019)
Petroleum wastewater sludge	–	–	–	–	116.69	(Mu et al., 2016)
Petroleum sludge	76.08	87.72	76.77	–	–	Present work

reaction (Kaur et al., 2018). The activation energy of PS during pyrolysis was estimated by employing three iso-conversional methods namely, KAS, OWF and Starink methods. The results for KAS, OWF and Starink methods are exhibited in Fig. 2a–c, respectively. The activation energy for different conversion (varying from 0.1 to 0.9) was calculated the slop of straight regression lines for different models. It was observed that as the conversion increased from 0.1 to 0.9, the slop of lines for different model also changed. As a result the activation energy also varied with conversion. The calculated values of activation energy at different conversion are given in Table 3 and the change in activation energy at different conversion for different model is depicted in Fig. 3. The average activation energy for KAS, OWF and Starink method was found to be 76.088, 87.427 and 76.779 kJ mol^{-1}, respectively, with correlation coefficient of 0.9897, 0.9937, and 0.9899, respectively. Comparable activation energy was obtained by all three methods. However, activation energy from OWF method was marginally higher that the other two methods (Fig. 3). Marginal difference for activation energy might be due to approximations and assumption followed during derivation of different models (Kaur et al., 2018). For instance, Doyle's approximation was followed during derivation of OWF method, while Starink and KAS do not adopt such approximation (Doyle, 1962; Yuan et al., 2017). The change in activation energy with conversion attributed to series of reactions with multi-stage kinetics during pyrolysis of PS. Thus, pyrolysis of PS is a complex process where every single reaction contributes totally or partly to the global reaction mechanism subject to degree of decomposition. Table 4 represents the comparative analysis of results obtained on activation energy during pyrolysis of PS form present work and published literatures based on iso-conversional models.

3.4. Determination of reaction kinetic model

Pyrolysis of PS is a complex process occurring through multiple parallel and series reactions. So, it is very challenging to find the reaction mechanism of such complex process. However, mechanistic model based on suitable mathematical approximation has been developed to predict the reaction mechanism of such complex processes. In the present study Z-master plot based on Criado method (Criado et al., 1989) was used to predict the mechanism during pyrolysis of PS.

The integral temperature term p(u) is a function of conversion and can be calculated by using activation energy obtained from iso-conversional method. In this work $p(u)/p(u_{0.5})$ is calculated using activation energy from Starink method. The plot of $p(u)/p(u_{0.5})$ versus conversion at different heating rate is shown in Fig. 4a. The nature of plot showed that different reaction mechanism could be followed at different conversion and heating rate during pyrolysis of PS. From conversion 0.1–0.3, 0.3–0.4, 0.4–0.5 and 0.5–0.6, the nature of plot is similar at all heating rate, while from conversion 0.6–0.9 drastic change in nature of plot was observed suggesting that different reaction mechanism would be followed at different heating rate. Thus, Fig. 4a illustrates that during pyrolysis of PS multiple kinetic model were followed depending on the level of conversion and heating rate during the process.

The Z-master plot at 5 K min^{-1} is shown in Fig. 4b. Based on the proximity of experimental and theoretical corves it was observed that reaction model depends on the degree of conversion. From conversion 0.1–0.2, 0.2–0.3, 0.4–0.5, 0.5–0.6, 0.6–0.7, 0.7–0.9 and 0.8–0.9, the model followed are F3/R1, R1, P4, D1, D4, R3, D2, respectively. The detail about the model has been given in Table S1. However, for conversion 0.3–0.4, the mechanism is not clear from

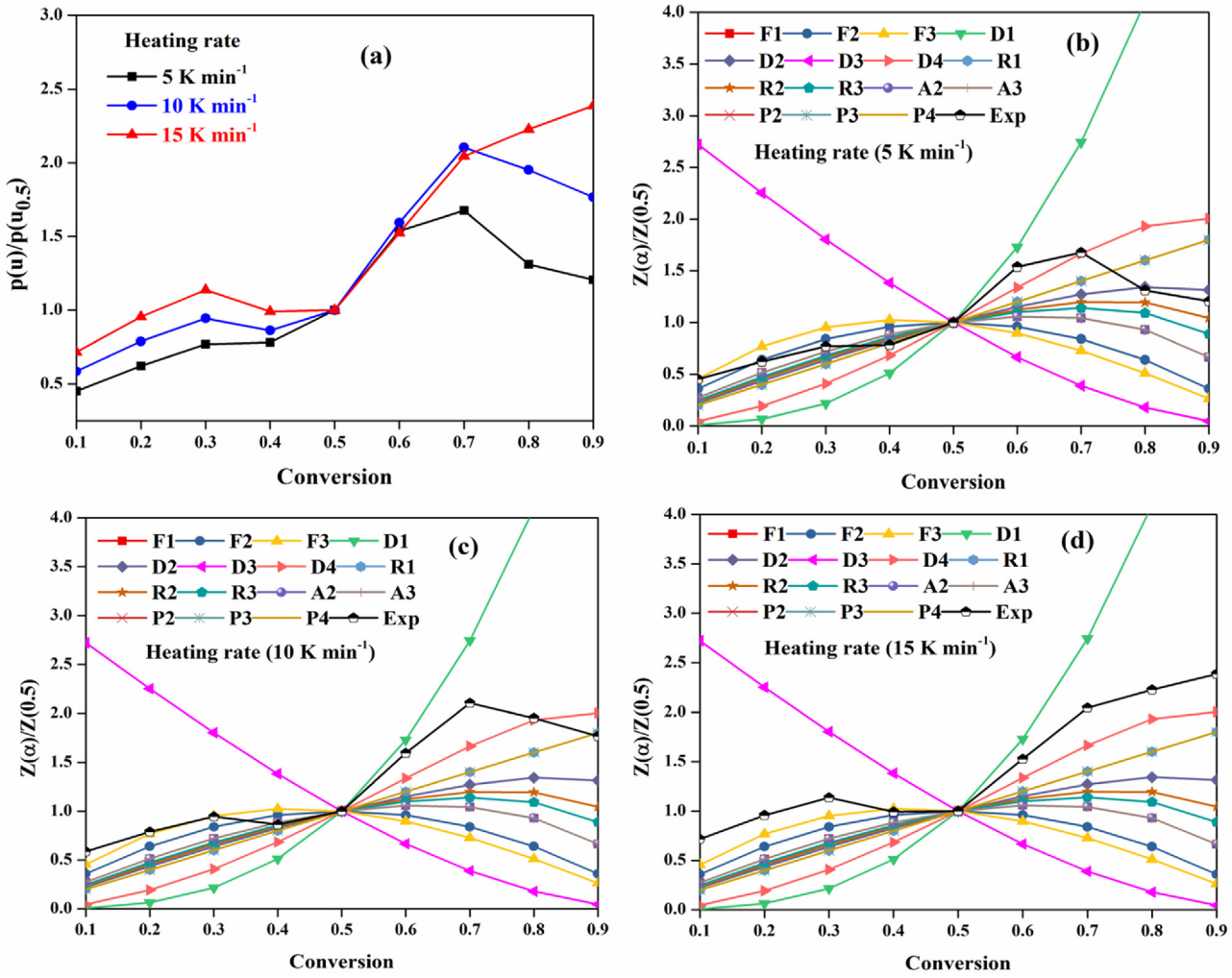

Fig. 4. **(a)** $p(u)/p(u_{0.5})$ versus conversion at different heating rates; **(b)** Z-master plot at 5 K min^{-1}; **(c)** Z-master plot at 10 K min^{-1}; **(d)** Z-master plot at 15 K min^{-1}.

Z-master plot. It is clear that at lower heating rate during pyrolysis of PS, prediction of solid reaction mechanism is very cumbersome. This might be reason for selection of intermediate or higher heating rate during prediction of solid reaction mechanism for pyrolysis of PS. The Z-master plot at 10 K min^{-1} is shown in Fig. 4c. From conversion 0.1–0.3, 0.3–0.4, 0.4–0.5, 0.5–0.7, and 0.7–0.9, the model followed are F3, F2, R3, D1, D4, respectively. The Z-master plot at 15 K min^{-1} is shown in Fig. 4d. From conversion 0.1–0.5, and 0.6–0.9, the model followed is F3 and D4, respectively. Qu et al. (Qu et al., 2019) and Miao et al. (Miao et al., 2019) investigated the reaction kinetic model for oil sludge at 60 K min^{-1} and 10 K min^{-1}, respectively, using Z-master plot method. They have studied the reaction kinetic model based on phase separation of oil sludge, while present work aimed to investigate the effect of heating rate on reaction model followed during pyrolysis.

3.5. Estimation of thermodynamic parameters

Table 5 represents the thermodynamic parameters for pyrolysis of PS. The thermodynamic parameters were calculated using the activation energy from Starink method. Also, the thermodynamic parameters were calculated at three different heating rates such as 5, 10, 15 K min^{-1}.

The frequency factor suggests the nature of complex formed during the pyrolysis of PS. The average values of frequency factor for pyrolysis of PS at 5, 10, 15 K min^{-1} was found to be 3.23×10^7, 1.30×10^7, 4.70×10^6 sec^{-1}, respectively. The value of frequency factor also varies with conversion. The lower value of frequency factor indicated the formation of closed complex while, higher value indicates the formation of simple complex during pyrolysis process (Kaur et al., 2018; Yuan et al., 2017). The large variation in frequency factor with conversion might be due to complex nature of pyrolysis of PS. The value of frequency factor also varies in accordance with activation energy. Lower value of frequency factor was obtained at lower activation energy, while higher value is observed at higher activation energy at given value of conversion.

The Enthalpy as a thermodynamic parameter defines the total heat content associated with system (Singh et al., 2020c). For pyrolysis of PS, it is the total heat absorbed by PS sample for converting into pyrolytic oil, gaseous product and char (Daugaard and Brown, 2003). The average change in enthalpy (Δ H) at 5, 10, 15 K min^{-1} was found to be 70.78, 70.52, 70.29 kJ mol^{-1}. Thus, positive value of Δ H revealed process is endothermic in nature and energy from external source is required for increasing the energy of PS reagent up to transition state for proceeding of pyrolysis process. Also, the effect of heating rate on Δ H during pyrolysis of PS is minimal. The value of Δ H also varied with conversion. At the start of reaction Δ H is small revealing the reactive system due to removal of moisture. The Δ H during pyrolysis suggested that the difference of energy between PS reagent and activated complex formed are matching with activation energy with slight difference. The lower difference between enthalpy and activation energy suggest that formation of

Table 5
Thermodynamic parameters at different heating rate based on activation energy from Starink method.

Conversion	Heating rate (5 K min^{-1})				Heating rate (10 K min^{-1})				Heating rate (15 K min^{-1})			
	A (s^{-1})	ΔH (kJ mol^{-1})	ΔG (kJ mol^{-1})	ΔS (J mol^{-1} K^{-1})	A (s^{-1})	ΔH (kJ mol^{-1})	ΔG (kJ mol^{-1})	ΔS (J mol^{-1} K^{-1})	A (s^{-1})	ΔH (kJ mol^{-1})	ΔG (kJ mol^{-1})	ΔS (J mol^{-1} K^{-1})
0.1	1.81×10^4	67.991	189.630	−0.172	1.32×10^4	67.883	200.909	−0.277	8.04×10^3	67.79862	213.9715	−0.298
0.2	8.16×10^6	101.182	188.156	−0.123	3.99×10^6	101.078	199.268	−0.185	1.69×10^5	100.997	212.160	−0.206
0.3	8.33×10^7	113.810	187.771	−0.104	3.49×10^7	113.699	198.834	−0.149	1.29×10^7	113.619	211.673	−0.169
0.4	2.00×10^8	118.342	187.645	−0.098	7.88×10^7	118.209	198.690	−0.131	2.76×10^7	118.130	211.511	−0.149
0.5	1.28×10^5	77.163	189.066	−0.158	8.28×10^4	76.895	200.284	−0.181	4.48×10^4	76.752	213.284	−0.195
0.6	2.79×10^2	43.870	191.279	−0.208	2.67×10^2	43.491	202.719	−0.217	2.05×10^2	43.220	215.946	−0.225
0.7	5.76×10^1	35.433	192.141	−0.222	6.06×10^1	34.983	203.659	−0.219	5.09×10^1	34.614	216.967	−0.224
0.8	5.69×10^1	35.073	192.148	−0.222	6.00×10^1	34.641	203.667	−0.210	5.04×10^1	34.177	216.975	−0.213
0.9	3.59×10^2	44.206	191.157	−0.208	3.38×10^2	43.805	202.585	−0.186	2.56×10^2	43.354	215.801	−0.190
Average	**3.23×10^7**	**70.785**	**189.888**	**−0.168**	**1.30×10^7**	**70.520**	**201.179**	**−0.195**	**4.70×10^6**	**70.295**	**214.254**	**−0.207**

activated complex during pyrolysis (Loy et al., 2018; Vlaev et al., 2007). That will facilitate the pyrolysis of PS.

The change in Gibbs free energy (Δ G) revealed the increase in energy of pyrolysis system as a result of activated complex (Kaur et al., 2018; Turmanova et al., 2008). The variation in Δ G with conversion at different heating rate is presented in Table 5. A positive Gibbs energy during pyrolysis of PS ascribed the unfavorable condition for reaction. That means system requires energy from external source to proceed (Mallick et al., 2018). The average change in Gibbs energy (Δ G) at 5, 10, 15 K min^{-1} was found to be 189.88, 201.17, 214.29 kJ mol^{-1}. The increase in average Δ G with heating rate revealed that pyrolysis process will consume more energy at higher heating rate.

The change in entropy measure the randomness or disorder of system. It is a state function of the system. The variation in Δ S with conversion at different heating rate is presented in Table 5. Result showed that for selected level of conversion at three different heating rates, the value of Δ S is negative revealing that during the pyrolysis PS sample is attaining a new state which is closer to thermodynamic equilibrium state as a result of randomness in products formed due breaking of bonds during pyrolysis. The average change in change in entropy (Δ S) at 5, 10, 15 K min^{-1} was found to be, – 0.168, – 0.195 and – 0.207 J mol^{-1} K^{-1}, respectively. The decrease in change in entropy with heating rate ascribed that at higher heating rate pyrolysis of PS is more favorable. The lower entropy during a process revealed that the sample has some chemical and physical changes due to which sample tend to attain new thermodynamic equilibrium state (Kaur et al., 2018; Yuan et al., 2017).

4. Conclusions and recommendations

The efficacy of petroleum sludge for energy potential was examined by performing pyrolysis of petroleum sludge using TGA analyzer at 5, 10, 15 K min^{-1} heating rate. The kinetic, thermodynamic parameters and solid reaction mechanism was investigated based on iso-conversional model (KAS, OWF and Starink) and Criado method (Z-master) plot. The average activation energy from KAS, OWF and Starink model was found to be 76.088, 87.426 and 76.779 kJ mol^{-1}. The lesser value of activation energy revealed the suitability of petroleum sludge for pyrolysis process. The close value of change in enthalpy and activation at different conversion facilitate the pyrolysis process by easier activated complex formation. The negative values of change in entropy (Δ S) at different level of conversion revealed that both chemical and physical changes during pyrolysis supporting the petroleum sludge sample to attain thermodynamic equilibrium state. The heating rate during pyrolysis has significant effect on thermodynamic parameter and solid reaction mechanism. Higher heating rate lowered the change in entropy as well as dual kinetic model (F3 for conversion < 0.5 and D4 for conversion > 0.5) was followed. However, at lower heating rate multiple kinetic model were followed depending on the degree of conversion. Although the future scope of pyrolysis process for treatment of petroleum sludge is very promising due to its fast and efficient nature, large treatment capacity, and high recovery of oil from petroleum sludge but moisture content of petroleum sludge is very high. Thus, it requires a pretreatment process to reduce its moisture content and make the process more efficient. Also, the cost of operation, maintenance of process reactor system, and energy input should be taken into consideration.

Overall, it may be concluded that in-depth analysis of kinetics, thermodynamics and solid reaction mechanism of pyrolysis of petroleum sludge makes the pyrolysis process more suitable for remediation and resource utilization by optimization and scale-up of process reactor system and make the process cost effective.

Declaration of Competing Interest

The authors report no declarations of interest.

Acknowledgment

Authors are grateful to the Department of Chemical Engineering and Technology and Central Instrument Facility Centre (CIFC), Indian Institute of Technology, (BHU) Varanasi, for conducting the work.

Appendix A. Supplementary data

Supplementary material related to this article can be found, in the online version, at doi:https://doi.org/10.1016/j.psep.2020.08.038.

References

Alam, M., Bhavanam, A., Jana, A., Viroja, Jk.S., Peela, N.R., 2020. Co-pyrolysis of bamboo sawdust and plastic: synergistic effects and kinetics. Renew. Energy 149, 1133–1145.
Al-Zahrani, S.M., Putra, M.D., 2013. Used lubricating oil regeneration by various solvent extraction techniques. J. Ind. Eng.Chem. 19 (2), 536–539.
Bach, Q.-V., Chen, W.-H., 2017. Pyrolysis characteristics and kinetics of microalgae via thermogravimetric analysis (TGA): a state-of-the-art review. Bioresour. Technol. 246, 88–100.
Aboulkas, A., El Harfi, K., 2008. Study of the kinetics and mechanisms of thermal decomposition of moroccan tarfaya oil shale and its kerogen. Oil Shale 25 (4).
Chen, J., Mu, L., Cai, J., Yao, P., Song, X., Yin, H., Li, A., 2015a. Pyrolysis and oxy-fuel combustion characteristics and kinetics of petrochemical wastewater sludge using thermogravimetric analysis. Bioresour. Technol. 198, 115–123.
Chen, J., Mu, L., Cai, J., Yin, H., Song, X., Li, A., 2015b. Thermal characteristics and kinetics of refining and chemicals wastewater, lignite and their blends during combustion. Energy Convers. Manage. 100, 201–211.
Chen, J., Mu, L., Jiang, B., Yin, H., Song, X., Li, A., 2015c. TG/DSC-FTIR and Py-GC investigation on pyrolysis characteristics of petrochemical wastewater sludge. Bioresour. Technol. 192, 1–10.
Chen, D., Shuang, E., Liu, L., 2018. Analysis of pyrolysis characteristics and kinetics of sweet sorghum bagasse and cotton stalk. J. Therm. Anal. Calorim. 131 (2), 1899–1909.
Cheng, S., Chang, F., Zhang, F., Huang, T., Yoshikawa, K., Zhang, H., 2018. Progress in thermal analysis studies on the pyrolysis process of oil sludge. Thermochim. Acta 663, 125–136.
Choudhury, D., Borah, R., Goswamee, R., Sharmah, H., Rao, P., 2007. Non-isothermal thermogravimetric pyrolysis kinetics of waste petroleum refinery sludge by isoconversional approach. J. Therm. Anal. Calorim. 89 (3), 965–970.
Choudhury, N.D., Bhuyan, N., Bordoloi, N., Saikia, N., Kataki, R., 2020. Production of bio-oil from coir pith via pyrolysis: kinetics, thermodynamics, and optimization using response surface methodology. Biomass Conv. Bioref, http://dx.doi.org/10.1007/s13399-020-00630-3.
Criado, J.M., 1978. Kinetic analysis of DTG data from master curves. Thermochim. Acta 24 (1), 186–189.
Criado, J., Malek, J., Ortega, A., 1989. Applicability of the master plots in kinetic analysis of non-isothermal data. Thermochim. Acta 147 (2), 377–385.
Daugaard, D.E., Brown, R.C., 2003. Enthalpy for pyrolysis for several types of biomass. Energy Fuels 17 (4), 934–939.
Dhyani, V., Kumar, J., Bhaskar, T., 2017. Thermal decomposition kinetics of sorghum straw via thermogravimetric analysis. Bioresour. Technol. 245, 1122–1129.
Doyle, C.D., 1962. Estimating isothermal life from thermogravimetric data. J. Appl. Polym. Sci. Symp. 6 (24), 639–642.
Gong, Z., Wang, Z., Wang, Z., Du, A., Fang, P., Sun, Z., Li, X., 2018. Study on pyrolysis of oil sludge with microalgae residue additive. The Canadian J. Chem. Eng. 96 (9), 1919–1925.
Gong, Z., Liu, C., Wang, M., Wang, Z., Li, X., 2020. Experimental study on catalytic pyrolysis of oil sludge under mild temperature. Sci.Total Environ. 708, 135039.
Gotor, F.J., Criado, J.M., Malek, J., Koga, N., 2000. Kinetic analysis of solid-state reactions: the universality of master plots for analyzing isothermal and non-isothermal experiments. J. Phys. Chem. A 104 (46), 10777–10782.
Heydari, M., Rahman, M., Gupta, R., 2015. Kinetic study and thermal decomposition behavior of lignite coal. Int. J. Chem. Eng. 2015.
Hu, G., Li, J., Zeng, G., 2013. Recent development in the treatment of oily sludge from petroleum industry: a review. J. Hazard. Mater. 261, 470–490.
Hu, J., Gan, J., Li, J., Luo, Y., Wang, G., Wu, L., Gong, Y., 2017. Extraction of crude oil from petrochemical sludge: characterization of products using thermogravimetric analysis. Fuel 188, 166–172.
Jiang, Y., Liu, Z., Zeng, G., Liu, Y., Shao, B., Li, Z., Liu, Y., Zhang, W., He, Q., 2018. Polyaniline-based adsorbents for removal of hexavalent chromium from aqueous solution: a mini review. Environ. Sci. Pollut. Res. 25 (7), 6158–6174.
Kaur, R., Gera, P., Jha, M.K., Bhaskar, T., 2018. Pyrolysis kinetics and thermodynamic parameters of castor (Ricinus communis) residue using thermogravimetric analysis. Bioresour. Technol. 250, 422–428.
Kumar, R., Strezov, V., Weldekidan, H., He, J., Singh, S., Kan, T., Dastjerdi, B., 2020. Lignocellulose biomass pyrolysis for bio-oil production: a review of biomass pre-treatment methods for production of drop-in fuels. Renew. Sustain. Energy Rev. 123, 109763.
Liu, J., Jiang, X., Zhou, L., Han, X., Cui, Z., 2009. Pyrolysis treatment of oil sludge and model-free kinetics analysis. J. Hazard. Mater. 161 (2), 1208–1215.
Liu, W., Luo, Y., Teng, Y., Li, Z., Ma, L.Q., 2010. Bioremediation of oily sludge-contaminated soil by stimulating indigenous microbes. Environ. Geochem. Health 32 (1), 23–29.
Loy, A.C.M., Gan, D.K.W., Yusup, S., Chin, B.L.F., Lam, M.K., Shahbaz, M., Unrean, P., Acda, M.N., Rianawati, E., 2018. Thermogravimetric kinetic modelling of in-situ catalytic pyrolytic conversion of rice husk to bioenergy using rice hull ash catalyst. Bioresour. Technol. 261, 213–222.
Ma, Z., Xie, J., Gao, N., Quan, C., 2019. Pyrolysis behaviors of oilfield sludge based on Py-GC/MS and DAEM kinetics analysis. J. Energy Inst. 92 (4), 1053–1063.
Mallick, D., Poddar, M.K., Mahanta, P., Moholkar, V.S., 2018. Discernment of synergism in pyrolysis of biomass blends using thermogravimetric analysis. Bioresour. Technol. 261, 294–305.
Miao, W., Li, X., Wang, Y., Lv, Y., 2019. Pyrolysis characteristics of oil-field sludge and the comparison of kinetic analysis with two representative methods. J. Pet. Sci. Eng. 182, 106309.
Mishra, G., Kumar, J., Bhaskar, T., 2015. Kinetic studies on the pyrolysis of pinewood. Bioresour. Technol. 182, 282–288.
Mu, L., Chen, J., Yao, P., Zhou, D., Zhao, L., Yin, H., 2016. Evaluation of co-pyrolysis petrochemical wastewater sludge with lignite in a thermogravimetric analyzer and a packed-bed reactor: pyrolysis characteristics, kinetics, and products analysis. Bioresour. Technol. 221, 147–156.
Poletto, M., Zattera, A.J., Santana, R.M.C., 2012. Thermal decomposition of wood: kinetics and degradation mechanisms. Bioresour. Technol. 126, 7–12.
Premarathna, K., Rajapaksha, A.U., Sarkar, B., Kwon, E.E., Bhatnagar, A., Ok, Y.S., Vithanage, M., 2019. Biochar-based engineered composites for sorptive decontamination of water: a review. Chem. Eng. J. 372, 536–550.
Qu, Y., Li, A., Wang, D., Zhang, L., Ji, G., 2019. Kinetic study of the effect of in-situ mineral solids on pyrolysis process of oil sludge. Chem. Eng. J. 374, 338–346.
Singh, B., Kumar, P., 2020. Pre-treatment of petroleum refinery wastewater by coagulation and flocculation using mixed coagulant: optimization of process parameters using response surface methodology (RSM). J. Water Process. Eng. 36, 101317.
Singh, S., Chakraborty, J.P., Mondal, M.K., 2019. Optimization of process parameters for torrefaction of Acacia nilotica using response surface methodology and characteristics of torrefied biomass as upgraded fuel. Energy 186, 115865.
Singh, S., Chakraborty, J.P., Mondal, M.K., 2020a. Pyrolysis of torrefied biomass: optimization of process parameters using response surface methodology, characterization, and comparison of properties of pyrolysis oil from raw biomass. J. Clean. Prod. 272, 122517.
Singh, S., Chakraborty, J.P., Mondal, M.K., 2020b. Torrefaction of woody biomass (Acacia nilotica): investigation of fuel and flow properties to study its suitability as a good quality solid fuel. Renew. Energy 153, 711–724.
Singh, S., Prasad Chakraborty, J., Kumar Mondal, M., 2020c. Intrinsic kinetics, thermodynamic parameters and reaction mechanism of non-isothermal degradation of torrefied Acacia nilotica using isoconversional methods. Fuel 259, 116263.
Soria-Verdugo, A., Goos, E., Morato-Godino, A., García-Hernando, N., Riedel, U., 2017. Pyrolysis of biofuels of the future: sewage sludge and microalgae–thermogravimetric analysis and modelling of the pyrolysis under different temperature conditions. Energy Convers. Manage. 138, 261–272.
Tian, Y., Li, J., Whitcombe, T.W., McGill, W.B., Thring, R., 2020. Application of oily sludge-derived char for lead and cadmium removal from aqueous solution. Chem. Eng. J. 384, 123386.
Turmanova, S.C., Genieva, S.D., Dimitrova, A.S., Vlaev, L.T., 2008. Non-isothermal degradation kinetics of filled with rise husk ash polypropene composites. Express Polym. Lett. 2, 133–146.
Vlaev, L.T., Georgieva, V.G., Genieva, S.D., 2007. Products and kinetics of non-isothermal decomposition of vanadium(IV) oxide compounds. J. Therm. Anal. Calorim. 88 (3), 805–812.
Vyazovkin, S., Burnham, A.K., Criado, J.M., Pérez-Maqueda, L.A., Popescu, C., Sbirrazzuoli, N., 2011. ICTAC Kinetics Committee recommendations for performing kinetic computations on thermal analysis data. Thermochim. Acta 520 (1–2), 1–19.
Xu, M., Zhang, J., Liu, H., Zhao, H., Li, W., 2014. The resource utilization of oily sludge by co-gasification with coal. Fuel 126, 55–61.
Yuan, X., He, T., Cao, H., Yuan, Q., 2017. Cattle manure pyrolysis process: kinetic and thermodynamic analysis with isoconversional methods. Renew. Energy 107, 489–496.
Zhong, J., Sun, X., Wang, C., 2003. Treatment of oily wastewater produced from refinery processes using flocculation and ceramic membrane filtration. Sep. Purif. Technol. 32 (1-3), 93–98.